

FIG. 2. Melting of lithium vs pressure.

in pressure and temperature. This empirical law was tested over a large compression range in the liquid and solid states in the present study on the alkali metals.

From the  $(\partial T/\partial P)_s$  measurements and compression measurements at high temperatures, the important Grüneisen parameter can be calculated from

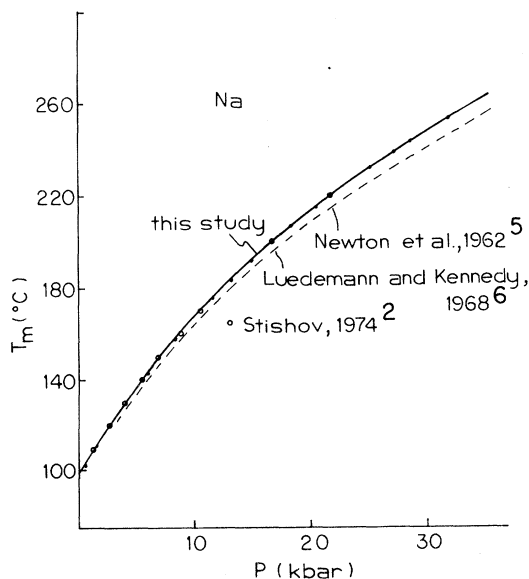


FIG. 3. Melting of sodium vs pressure.

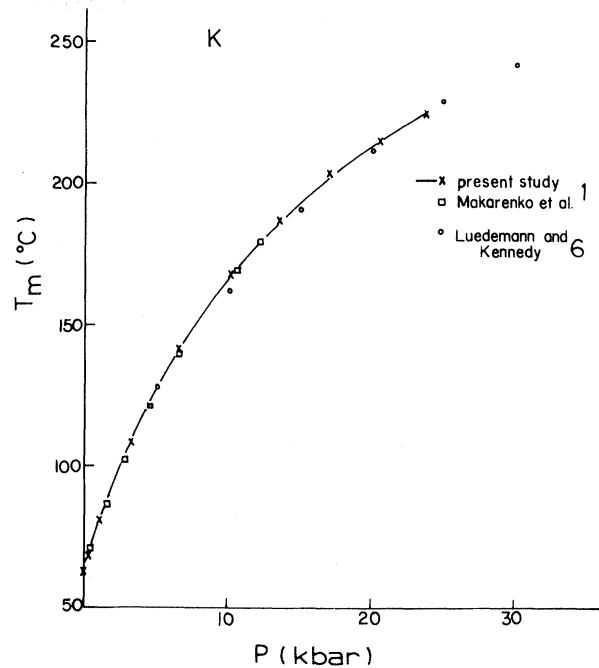


FIG. 4. Melting of potassium vs pressure.

$$\gamma = (B_s/T)(\partial T/\partial P)_s, \quad (2)$$

where  $B_s$  is the adiabatic bulk modulus. The behavior of  $\gamma$  at high compression is discussed.

#### APPARATUS

The measurements were made in an end-loaded piston-cylinder apparatus with an inner diameter of 19 mm and a length of 100 mm. The high-pressure cell is shown in Fig. 1. A 1:1 mixture of pentane and isopentane was used as the hydrostatic pressure medium. The top pressure seal consists of a conical plug with a steel wedge ring and rubber gasket. Sheathed wires soldered into steel cones were used for the electrical feedthrough. This seal assembly is very reliable and there is no evidence of leakage or failure in any of the experiments. The bottom seal is a modified Bridgman seal with low and almost constant friction of about 0.7 kbar. The sample is located in a thin-walled stainless-steel capsule with a movable lid. No chemical reaction of the steel and the alkali metals was observed. The capsule is surrounded by a wire-wound heater and thermally insulating glass ceramic.

#### PRESSURE AND TEMPERATURE MEASUREMENT

The resistance of a manganin wire inside the pressure chamber was recorded as a function of applied

pressure for a compression-decompression cycle. From this the gauge factor is determined and the pressure changes can be measured. The details of this procedure are described by Bohler *et al.*<sup>4</sup>

For the measurement of the temperature and  $\Delta T$ , we used sheathed Chromel-Alumel thermocouples with a wire diameter of 0.1 mm and a stainless-steel sheath diameter of 0.5 mm. The stainless-steel sheath prevented chemical contamination and plastic deformation of the thermocouple wires.

### MELTING

The melting temperature as a function of pressure was measured with one thermocouple which was located approximately in the geometric center of the sample. Melting and freezing could be easily observed by monitoring the temperature during melting and freezing on a strip chart recorder. The thermocouple voltage and the resistance of the manganin gauge were recorded simultaneously at the temperature rests during melting or freezing. The reproducibility of the measurement was within 0.5°C. Melting points and freezing points fell within this precision. The pressure correction of Chromel-Alumel thermocouples in the pressure and temperature range of this study is very close to zero and the uncertainty in the melting-point measurements is therefore less than  $\pm 0.25^\circ\text{C}$ . The uncertainty in pressure is  $\pm 0.4\%$ , which is based on the uncertainty in the estimate of the dilation of the pressure chamber.

### $(\partial T/\partial P)_S$ , MEASUREMENT

The adiabat measurement used the same apparatus as was used for the melting experiments. The measurement of the adiabats,  $(\partial T/\partial P)_S$ , is essentially the measurement of a temperature change in a sample during a rapid incremental change in pressure. This is achieved by opening a valve connecting the piston ram with a secondary high-pressure reservoir for a very short time. The time period of a typical pressure change is less than one-tenth of a second, so heat loss during the pressure pulse can be neglected. The measurement is therefore very close to adiabatic. Pressure changes of a few tenths of a kilobar are sufficient to generate voltage signals from the thermocouple of several tens of microvolts. For the alkali metals, the values of  $(\partial T/\partial P)_S$  are several degrees per kilobar. During adiabatic compression, the voltage change of the thermocouple and the resistance change of the manganin wire are recorded simultaneously on a strip chart recorder. The accuracy in  $(\partial T/\partial P)_S$  is about  $\pm 1\%$ .

TABLE I. Melting temperature  $T_m$  of Li, Na, and K at high pressures. 1-atm handbook values in brackets.

P (kbar)	$T_m$ ( $^\circ\text{C}$ )		
	Li	Na	K
0	180.0 (180.5)	97.8 (97.5)	63.7 (63.3)
5	194.8	136.5	128
10	205.9	167.5	167
15	215.2	192.5	195
20	223.0	214.0	214
25	229.3	232.5	229
30	234.8	249.0	

### SAMPLES

All samples were of a purity of at least 99.5%. Sodium with a purity of  $>99.5\%$  was purchased from Baker Chemical Co., 99.9%-pure lithium from Mackay Inc., and 99.5%-pure potassium from Research Organic/Inorganic Chemical Corp. The samples were cut and filled in the stainless-steel capsule under mineral oil.

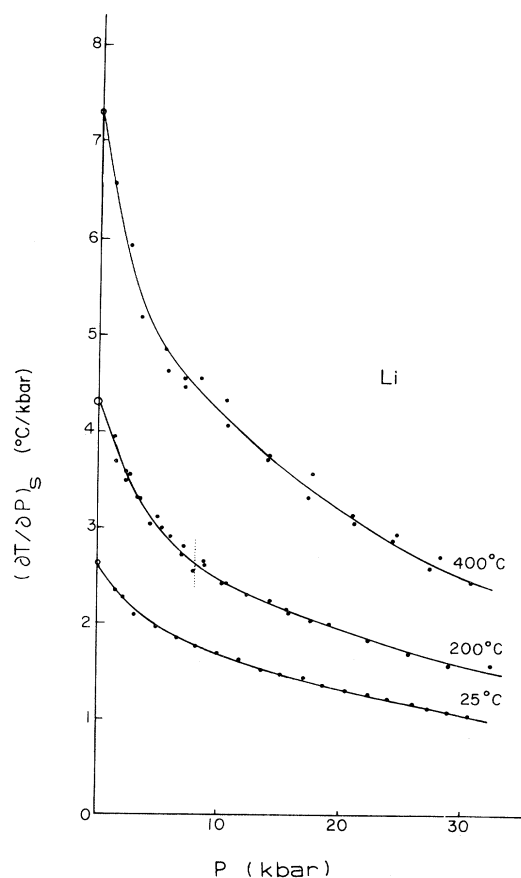


FIG. 5. Adiabats of lithium as a function of pressure and temperature.

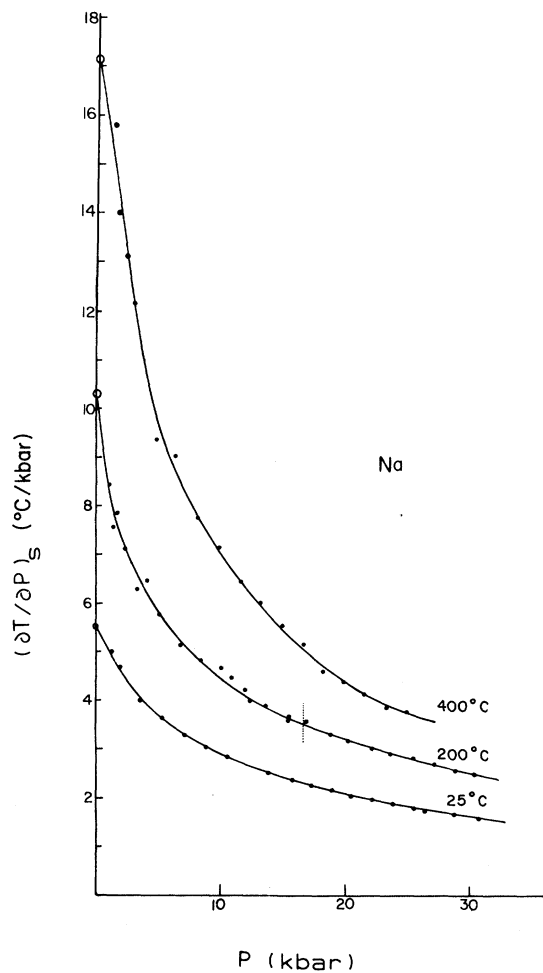


FIG. 6. Adiabats of sodium as a function of pressure and temperature.

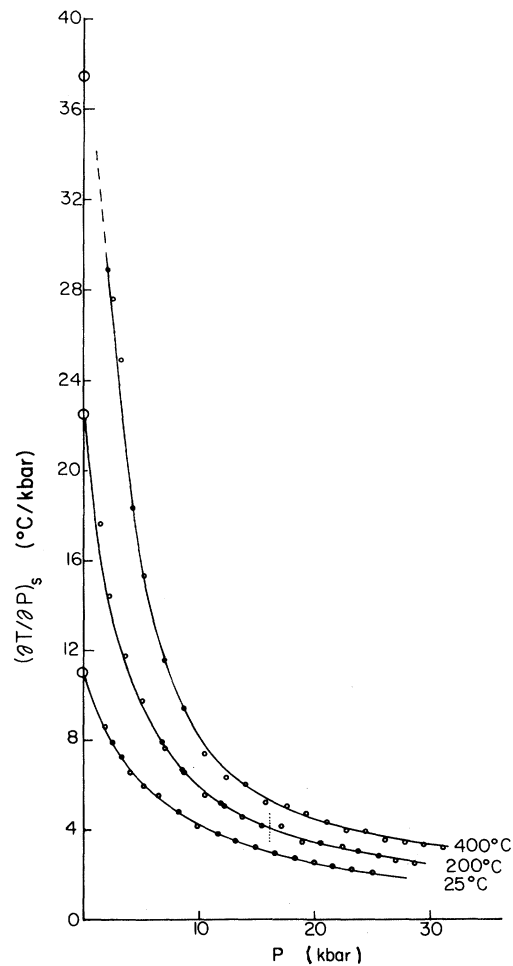


FIG. 7. Adiabats of potassium as a function of pressure and temperature.

TABLE II. Values of  $(\partial T/\partial P)_s = \alpha T/c_p \rho$  of Li, Na, and K at 1 atm.

	$T$ (K)	$\alpha$ ( $10^{-4} \text{ deg}^{-1}$ ) <sup>a</sup>	$c_p$ ( $10^{-3} \text{ kbar cm}^3 \text{ deg}^{-1} \text{ g}^{-1}$ ) <sup>b</sup>	$\rho$ ( $\text{g/cm}^3$ )	$(\partial T/\partial P)_s$ (deg/kbar)
Li	298	1.58	35.7	0.534	2.44
	473	1.96	43.6	0.507	4.19
	673	2.06	42.1	0.495	6.66
Na	298	2.08	12.3	0.970	5.21
	473	2.63	13.4	0.903	10.3
	673	2.78	12.8	0.856	17.1
K	298	2.46	7.56	0.860	11.3
	473	3.00	7.90	0.795	22.6
	673	3.18	7.64	0.748	37.5

<sup>a</sup>Reference 8.

<sup>b</sup>Reference 9.

## RESULTS

The melting and freezing temperatures were measured during a compression-decompression cycle. Hence drift in the thermocouple output and possible contamination of the samples can be checked. No differences larger than 0.5°C between the melting temperature taken at increasing pressure and those taken at decreasing pressure were observed. For accurate pressure estimates the pressure coefficient of the manganin gauge resistance was obtained from the compression-decompression cycle along the melting curves. The results are shown in Figs. 2–4 and compared with previous measurements. Perfect agreement with the measurements by Stishov and co-workers<sup>1,2</sup> is observed, whereas older measurements using nonhydrostatic pressure cells show strong deviation from our measured values.<sup>5,6</sup> The values given in Table I are taken from the smoothed curves in the Figs. 2–4. The melting points measured at 1 atm show good agreement with handbook values.

The results of the  $(\partial T/\partial P)_s$  measurements are shown in the Figs. 5–7 as a function of pressure and temperature. Our results for Na and K at room temperature are essentially identical to those measured by Ramakrishnan and Kennedy.<sup>7</sup> Each data point represents one pressure pulse and  $\Delta T/\Delta P$  is taken as  $(\partial T/\partial P)_s$ . The nature of the high-pressure seal and the friction makes the measurement of  $(\partial T/\partial P)_s$  below 1 kbar impossible. The  $(\partial T/\partial P)_s$  curves were therefore extrapolated to 1-atm values calculated from

$$\left[ \frac{\partial T}{\partial P} \right]_s = \frac{\alpha T}{c_p \rho}, \quad (3)$$

where  $\alpha$  is the thermal-expansion coefficient,  $c_p$  is the specific heat at constant pressure, and  $\rho$  is the density. Results and data sources are given in Table II. The uncertainty in  $\alpha$  is probably on the order of

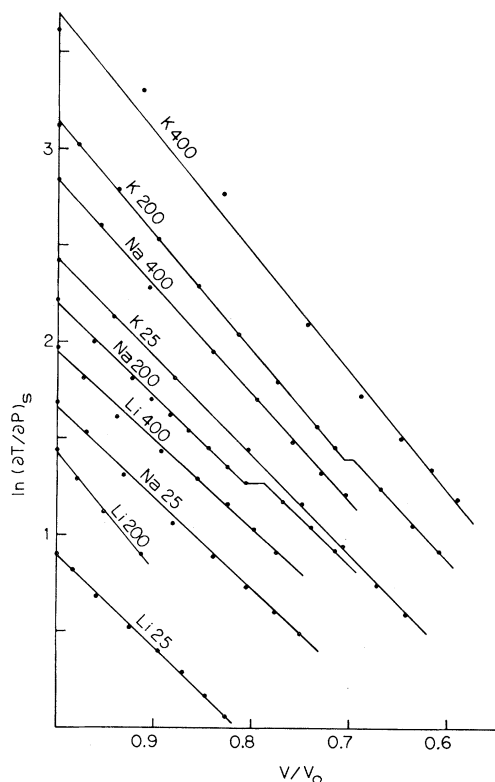


FIG. 8. Volume dependence of  $\ln(\partial T/\partial P)_s$ . The points are taken from the smoothed curves in Figs. 5–7.  $V/V_0$  was set equal to 1 at 1 atm for all temperatures.

several percent, but our curves and the calculated 1-atm intercepts are in good agreement considering the steepness of the curves at low pressure and high temperature. At 25°C all three alkali metals are in the solid phase and at 400°C they are in the liquid phase. The dashed lines on the 200°C curves represent the liquid-solid phase transitions. Changes of  $(\partial T/\partial P)_s$  at the transition larger than the data scatter were not observed for any of the three alkali metals. Table III lists the values of  $(\partial T/\partial P)_s$  taken

TABLE III. Values of  $(\partial T/\partial P)_s$  in deg/kbar taken from smoothed curves.

P (kbar)	T (°C)	Li			Na			K		
		25	200	400	25	200	400	25	200	400
0 <sup>a</sup>		2.44	4.20	7.2	5.40	10.3	17.1	11.3	22.6	37.5
2		2.27	3.62	6.10	4.60	7.45	13.5	8.4	15.0	27.0
5		1.95	3.05	4.85	3.70	5.90	10.2	6.1	9.7	16.0
10		1.68	2.47	4.17	2.90	4.55	7.3	4.2	5.9	8.1
15		1.49	2.17	3.63	2.44	3.75	5.6	3.2	4.3	5.6
20		1.33	1.95	3.20	2.08	3.20	4.5	2.55	3.4	4.5
25		1.19	1.75	2.81	1.82	2.83	3.7	2.1	2.9	3.8
30		1.06	1.58	2.48	1.63	2.52	3.2	1.8	2.5	3.3

<sup>a</sup>See Table II.

TABLE IV. Bulk moduli and their isothermal pressure and temperature derivatives of Li, Na, and K.

	$B_0^a$ (kbar)	$dB_0/dT^b$ ( $10^{-2}$ kbar deg $^{-1}$ )	$B_0'^a$	$dB_0'/dT^b$ ( $10^{-3}$ deg $^{-1}$ )
Li	112.7±6	-11.2 <sup>c</sup>	3.58±0.1	1.0 <sup>c</sup>
Na	62.1±3	-4.3±0.5	3.86±0.05	1.2±0.3
K	30.9±1	-2.5±0.5	3.83±0.02	1.3±0.3

<sup>a</sup>Average values from Bridgman (Ref. 11), Vaidya *et al.* (Ref. 12), and Grover *et al.* (Ref. 13).

<sup>b</sup>From  $B_{\text{average}}$  at room temperature and  $B$  at 200°C by Makarenko *et al.* (Ref. 2).

<sup>c</sup>Extrapolation of Bridgman's data (Ref. 10).

from the graphically smoothed curves in Figs. 5–7.

It has been shown in a previous study<sup>3</sup> that the adiabats of materials with high compressibility decrease as a function of density with a power

$$n = -\partial \ln(\partial T/\partial P)_s / \partial \ln \rho, \quad (1')$$

where  $n$  is only moderately temperature dependent. The quality of the fit of the experimental data to such a functional dependence of  $(\partial T/\partial P)_s$  can be checked for the alkali metals, where large decreases of  $(\partial T/\partial P)_s$  over a large compression range are found. The only compression data at high temperature for Li are available from Bridgman<sup>10</sup> to 95°C and for Na and K from Makarenko *et al.*<sup>2</sup> to 200°C. For the present study the pressure-volume data was fit to a first-order Birch equation of the form

$$P = \frac{3}{2} B_0 [(V_0/V)^{7/3} - (V_0/V)^{5/3}] \times [1 + \frac{3}{4} (B_0' - 4)(V_0/V)^{2/3} - 1], \quad (4)$$

where  $B_0$  is the isothermal bulk modulus at 1 atm and  $B_0'$  is its pressure derivative. From this, the temperature dependence of  $B_0$  and  $B_0'$  was calculated. The results are shown in Table IV.

The compression as a function of pressure and temperature was calculated from Eq. (4). Values for  $B_0$  and  $B_0'$  at 400°C were obtained from a linear extrapolation of  $B_0$  and  $B_0'$  in  $T$ .

For Li, Na, and K, a least-squares fit to a straight line of the experimental data to

$$\ln(\partial T/\partial P)_{s,P} = \ln(\partial T/\partial P)_{s,P=0} + m (V/V_0) \quad (5)$$

yields significantly better fits than using Eq. (1). The results are shown in Table V.

In Fig. 8 the logarithm of  $(\partial T/\partial P)_s$  of Li, Na, and K is plotted versus the compression calculated from Eq. (4).  $V/V_0$  was set equal to 1 at 1 atm for all temperatures. The volume changes at the liquid-solid transition for Na and K at 200°C were taken from Makarenko *et al.*<sup>2</sup> The quality of the fit is represented by the standard deviations of the slope in Table V.

The Grüneisen parameter  $\gamma$  was calculated from

$$\gamma = (B_s/T)(\partial T/\partial P)_s.$$

Adiabatic bulk modulus data,  $B_s = -V(\partial P/\partial V)_s$ , however, are not available for the alkali metals at high temperatures. Therefore, a correction for the isothermal bulk modulus has to be applied using

$$B_s = B_T + TC_V \gamma^2 / V, \quad (6)$$

where  $C_V$  is the specific heat at constant volume, and  $V$  is the molar volume.  $\gamma$  can then be calculated from Eqs. (6) and (2):

$$\gamma = B_T(\partial T/\partial P)_s / T + C_V(\partial T/\partial P)_s \gamma^2 / V. \quad (7)$$

Equation (7) is solved for  $\gamma$  using  $B_T$  values as shown in Table IV and by assuming constant Dulong-Petit values for  $C_V$ .  $C_V$  is most probably not constant at high temperatures, especially for the liquid, but the above assumption is reasonable when  $C_V$  is used as a correction term for the calculation of  $\gamma$ . The results are shown in Table VI and Fig. 9 as a function of pressure and temperature and in Fig. 10

TABLE V. Volume dependence of the adiabat  $(\partial T/\partial P)_s$  of Li, Na and K. The data in Table III were least-squares-fitted to  $\ln(\partial T/\partial P)_{s,P} = \ln(\partial T/\partial P)_{s,P=0} + m (V/V_0)$ .

$T$ (°C)	$(\partial T/\partial P)_{s,P=0}$ (deg/kbar)			$m$		
	25	200	400	25	200	400
Li	2.44	4.14	6.90	4.76±0.07	6.10±0.27	4.51±0.14
Na	5.26	8.84	17.02	4.78±0.09	4.72±0.06	5.57±0.06
K	11.3	23.1	41.8	5.11±0.04	5.94±0.05	6.25±0.21

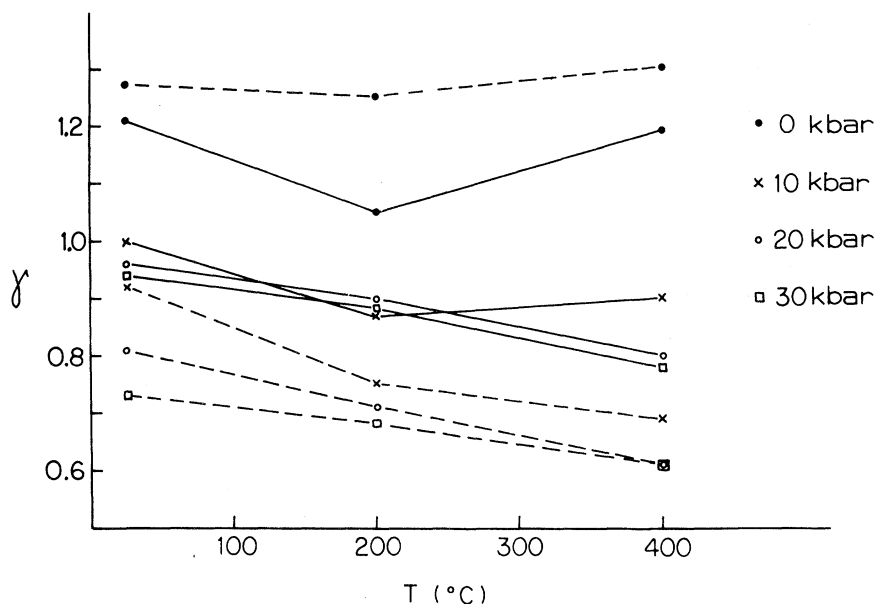


FIG. 9. Grüneisen parameter of sodium and potassium as a function of temperature along isobars. The solid lines are for sodium and the dashed lines for potassium.

as a function of compression along isotherms. The uncertainty in  $\gamma$  is due to the uncertainty in the bulk modulus and is about 10%.

#### DISCUSSION

The use of hydrostatic pressure cells with internal pressure gauges and thermocouples located directly in the sample yields the melting temperature as a function of pressure with high accuracy. For Na and Li, strong deviations from the results of older measurements using nonhydrostatic pressure cells are observed. The agreement of the present measurements with those of Stishov and co-workers is excellent and their pressure range is more than doubled with no considerable increase in uncertainties in pressure and temperature. The pressure apparatus used in this study is capable of working to 40 kbar but the approximately 32-kbar yield strength of the steel parts used for the high-pressure seals and the steel liner (see Fig. 1) preclude a routine measurements over 32 kbar.

The liquid-solid transition does not change the value of the adiabat or the slope of the adiabat-pressure curves. In contrast,  $(\partial T/\partial P)_s$  exhibits large changes through the phase changes of KBr, RbCl, Ce, and Bi.<sup>14</sup> Very small structural changes from the solid to the liquid phase also exhibited as small volume changes of 1–2% at the transition could explain the very small shift in  $(\partial T/\partial P)_s$  at the transition.

One of the objectives of this study was to examine

the nature of the behavior of the adiabat with volume. Previously a simple relationship of  $(\partial T/\partial P)_s$  with volume was observed [Eq. (1)]. Based on  $(\partial T/\partial P)_s$  measurements on olivine and magnesium oxide, this relationship was applied to calculate the adiabatic gradient in the deep mantle of the earth. This yielded good agreement with theoretical results.<sup>3</sup> Because Li, Na, and K have such high compressibilities, such a functional depen-

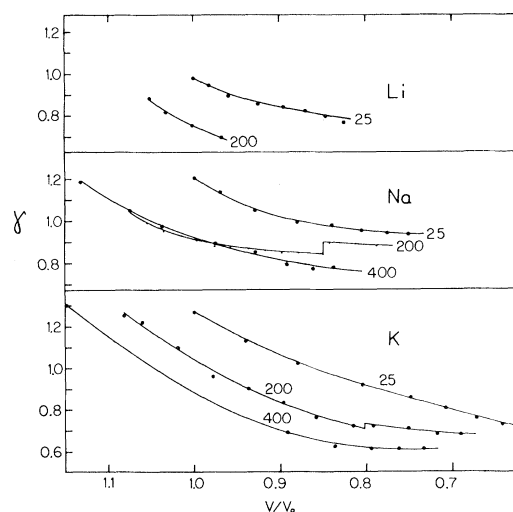


FIG. 10. Grüneisen parameter as a function of compression along isotherms. The temperatures are in degrees centigrade. The jumps at 200°C represent the liquid-solid transitions.

TABLE VI. Pressure and temperature dependence of the Grüneisen parameter of Li, Na, and K. Values marked with an asterisk are in the liquid state.

$P$ (kbar) \ $T$ (°C)	Li			Na			K		
	25	200	400	25	200	400	25	200	400
0	0.98	0.89*		1.21	1.05	1.19*	1.27	1.25	1.30*
5	0.90	0.75*		1.05	0.90	0.97*	1.02	0.89	0.98*
10	0.85	0.70		1.00	0.87	0.90*	0.92	0.75	0.69*
15	0.84	0.69		0.98	0.85	0.85*	0.86	0.72	0.62*
20	0.82	0.69		0.96	0.90*	0.80*	0.81	0.71*	0.61*
25	0.80	0.68		0.94	0.89*	0.77*	0.76	0.68*	0.61*
30	0.76	0.67		0.94	0.88*	0.78*	0.73	0.68*	0.61*

dence can be examined for compressions up to 40%. It is evident from Fig. 8 that a simple relationship such as Eq. (5) is a good representation of the behavior of  $(\partial T/\partial P)_s$ . Equation (5) yielded significantly better fits than Eq. (1). The advantage of such a method of fitting  $(\partial T/\partial P)_s$  data is obvious. The linear relation between  $\ln(\partial T/\partial P)_s$  and volume allows the extrapolation to higher pressures and the consistency in the slopes can be used to extrapolate to higher temperatures. A comparison with theoretical predictions for the adiabat at high pressures and high temperatures might be useful. It is interesting to note that the bulk modulus of metals shows a similar functional dependence of the volume<sup>15</sup> as the adiabat.

The present study is the first experimental estimate of the Grüneisen parameter  $\gamma$  at high pressures and high temperatures for solid and liquid alkali metals. The volume dependence of  $\gamma$  as shown in Fig. 10 shows a significant deviation from the often assumed power-law equation

$$\gamma = \gamma_0 (V/V_0)^q \quad (8)$$

A fit of the calculated  $\gamma$  values to Eq. (8) yields values of  $q$  close to 1, and therefore a very close to linear  $\gamma$ -volume dependence. The highest uncertainty in the calculation of  $\gamma$  is in the large uncertainty in the bulk modulus. The lack of accurate values of the adiabatic bulk modulus  $B_s$  from ultrasonic measurements at high pressures and high temperatures requires the use of isothermal bulk modulus data. These are obtained by fitting isothermal compression measurements to a Birch equation, which is derived from the theory of finite strain. The Birch equation is believed to be one of the best equations of state for alkali metals.<sup>15</sup> From this, a reasonable

uncertainty in the bulk modulus at a compression of 40% is about  $\pm 10\%$ , which leads to the same uncertainty in  $\gamma$ , and the uncertainty in the zero-pressure bulk modulus, as shown in Table IV, is due to the variation of the compression data from different sources.

In summary, several properties of the pressure dependence of  $\gamma$  have been observed: (1)  $\gamma$  decreases with pressure for both solid and liquid Li, Na, and K. This is in contrast to some organic fluids, and for mercury and water, where a strong increase of  $\gamma$  with compression is observed<sup>16</sup>; (2)  $\gamma$  increases at the liquid-solid transition by 7% for Na and by 4% for K. No compression data through the liquid-solid transition for Li were found; (3) the  $\gamma$ -volume curves show strong curvature with  $\gamma$  becoming less volume dependent at high compression; (4) at constant pressure,  $\gamma$  decreases with temperature except for Na and K at 1 atm, where  $\gamma$  increases between 200 and 400°C (see Fig. 9). The slopes of the  $\gamma$  curves vary between  $3 \times 10^{-4}$  and  $6 \times 10^{-4}$  deg<sup>-1</sup>; (5) at constant volume,  $\gamma$  decreases with temperature (see Fig. 10); (6) the initial slopes of the  $\gamma$ -volume curves vary between 2 and 3.5. At high compression  $\gamma$  tends to approach asymptotic values of about 0.6–0.7.

#### ACKNOWLEDGMENTS

Thanks are due to Jimmie Yamane for the machining of the parts and the upkeep of the high-pressure apparatus. The author gratefully acknowledges support from the National Science Foundation Grant No. EAR-80-10827, Department of Energy Grant No. DE-AT03-81ER, and financial support from the Lawrence Livermore National Laboratories Grant No. LLNL-4145105.

<sup>1</sup>I. N. Makarenko, A. M. Nikolaenko, and S. M. Stishov, *High Pressure Science and Technology, Sixth AIRAPT Conference (1977)* 347, edited by K. D. Timmerhaus

and M. S. Barber (Plenum, New York, 1979).

<sup>2</sup>I. N. Makarenko, A. M. Nikolaenko, and S. M. Stishov, *Liquid Metals* **30**, 79 (1976).



- <sup>3</sup>R. Boehler, *J. Geophys. Res.* 87, 5501 (1982).
- <sup>4</sup>R. Boehler, I. C. Getting, and G. C. Kennedy, *J. Phys. Chem. Solids* 38, 233 (1977).
- <sup>5</sup>R. C. Newton, A. Jayaraman, and G. C. Kennedy, *J. Geophys. Res.* 67, 2559 (1962).
- <sup>6</sup>H. D. Luedemann and G. C. Kennedy, *J. Geophys. Res.* 73, 2795 (1962).
- <sup>7</sup>J. Ramakrishnan and G. C. Kennedy, *J. Phys. Chem. Solids* 41, 301 (1980).
- <sup>8</sup>E. I. Gol'tsova, *High Temp.* 4, 348 (1966).
- <sup>9</sup>R. A. Robie, B. S. Hemingway, and J. R. Fisher, *Geological Survey Bulletin 1492*, (U. S. GPO, Washington, D. C., 1978), pp. 66, 69, and 75.
- <sup>10</sup>P. W. Bridgman, *Phys. Rev.* 3, 153 (1914).
- <sup>11</sup>P. W. Bridgman, *Proc. Am. Acad. Arts Sci.* 76, 55 (1948).
- <sup>12</sup>S. N. Vaidya, I. C. Getting, and G. C. Kennedy, *J. Phys. Chem. Solids* 32, 2545 (1971).
- <sup>13</sup>R. Grover, R. N. Keeler, F. J. Rogers, and G. C. Kennedy, *J. Phys. Chem. Solids* 30, 2091 (1969).
- <sup>14</sup>J. Ramakrishnan, R. J. Hardy, and G. C. Kennedy, *J. Phys. Chem. Solids* 40, 297 (1979).
- <sup>15</sup>R. Grover, I. C. Getting, and G. C. Kennedy, *Phys. Rev. B* 7, 567 (1973).
- <sup>16</sup>R. Boehler and G. C. Kennedy, *J. Appl. Phys.* 48, 4183 (1977).